Inorganic Chemistry

Article

pubs.acs.org/IC

Substituent Effects on the Biological Properties of Zn-Salophen Complexes

Ilaria Giannicchi,[†] Rosa Brissos,[‡] David Ramos,[§] Joaquin de Lapuente,[§] João Carlos Lima,[∥] Antonella Dalla Cort,*[,†] and Laura Rodríguez*[,‡]

[†]Dipartimento di Chimica and IMC-CNR Sezione Meccanismi di Reazione, Università La Sapienza, Box 34 Roma 62, 00185 Roma, Italy

[‡]Departament de Química Inorgànica, Universitat de Barcelona, Martí i Franquès 1-11, 08028 Barcelona, Spain

[§]Unitat de Toxicologia Experimental i Ecotoxicologia, Parc Científic de Barcelona, c/Baldiri i Reixach, 10-12, 08028 Barcelona, Spain

[∥]REQUIMTE, Departamento de Química, Faculdade de Ciências e Tecnologia, Universidade Nova de Lisboa, 2829-516 Monte de Caparica, Portugal

Supporting Information

ABSTRACT: The synthesis, characterization, and luminescent properties of a series of 5,5′-X-substituted salophen ligands, X= OCH_3, Br, and NO_2, and the corresponding Zn(II) complexes are reported here. Their biological activity has been analyzed and related to the different Lewis acid character of the complexes. In vitro studies (AFM and absorption and emission titrations) show that the strongest interaction with free plasmid DNA is observed for 5,5′-dinitro-substituted Zinc-salophen complex **3b**. Semiempirical theoretical calculations together with redox potential measurements suggest that this might be interpreted as a direct consequence of this compound having the hardest Lewis acid character. Cellular uptake and cytotoxicity studies undertaken with these metal complexes show that they enter the cells but are not cytotoxic.

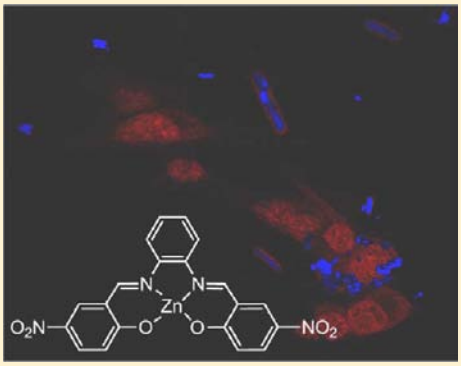

INTRODUCTION

Metallo-salen/salophen (metal complexes of bis(salicylidene)-ethylenediamine and bis(salicylidene)diphenyldiamine) complexes are well established efficient catalysts in organic chemistry because of their rich redox chemistry and ease of manipulation.[1−4] Furthermore, biochemists have utilized the oxidative nature of metallo-salen complexes to develop novel DNA/RNA modifiers and biomolecular probes.[5−7] The ultimate cytotoxicity of such metal complexes depends on a number of factors, including the mode of cellular interaction, transport/cellular-uptake potential, intrinsic structure, and reactivity of the compounds.[8−11] The cellular-interaction and apoptotic activity of the metallo-salen complexes appears to be highly dependent on the nature of the central metal ion and the substituents present on the salen moiety.[12−14]

The redox properties of sal(oph)en-containing coordination compounds have been used in biological studies that revealed their involvement in metal-dependent DNA-damage processes.[15,16] Indeed, Fe(III)- and Mn(III)-salen/salophen complexes show cytotoxicity and effective DNA damage, inducing apoptosis in cultured human cells.[17] Some lanthanide-salophen complexes are able to bind neutral sugars and lipids, including lysophosphatidic acid (a biomarker for several pathological conditions including ovarian cancer).[18]

The nonredox metal-ion zinc(II) salen/salophen-type complexes are also relevant because zinc is the second most abundant transition metal in living organisms after iron, and it is the only metal that appears in all enzyme classes.[15] It has been observed that in general the lack of redox activity of Zn(II) normally leads to Zn-salen/salophen compounds that do not show cytotoxic properties.[15,19,20] This, together with the closed-shell d^{10} configuration featured by the metal, make such complexes ideal candidates for the generation of biological fluorescence probes and ligand-dependent fluorescence materials.[21−23]

It has been established that the nature and position of the substituents on the ligand skeleton, solubility, and cellular permeability play a critical role in determining their cytotoxic behavior.[12,24] S. Mandal and co-workers described the diverse apoptotic activity displayed by Mn(III)-salen/salophen derivatives decorated with methoxy or hydroxyl groups.[17] However, no straightforward correlation with the nature of the substituent was clearly established. However, the bridging group, which is ethylenediamine in the case of salen and an *o*-phenylenediamine unit for salophen derivatives, also seems to have an effect.

Recently, we reported the biological study of two Zn(II)-salophen complexes that differ in their bridging unit.[19] They both display high IC_{50} values, but they partially differ for their

Received: February 19, 2013
Published: July 29, 2013

   dx.doi.org/10.1021/ic4004356 | *Inorg. Chem.* 2013, 52, 9245−9253

cytotoxicity in cells. Thanks to their intrinsic luminescent properties, we proposed them to be potentially good candidates for use as fluorescent markers in cells.

In this study, we focused our attention on a series of 5,5′-X-substituted Zn(II)-salophen derivatives, X =OCH_3, Br, and NO_2 (Chart 1), monitoring their biological behavior with

Chart 1

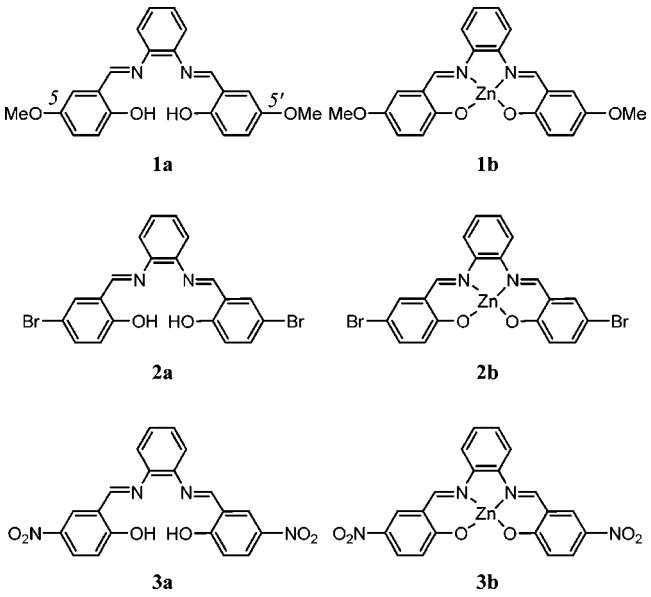

respect to the different nature of the substituent. Analogous studies with the uncomplexed ligands were performed for comparison purposes.

EXPERIMENTAL SECTION

General Information. The best commercially available chemicals were obtained and used without further purification unless otherwise stated. pBR322 plasmid DNA was obtained from Boehringer-Mannheim (Mannheim, Germany). HEPES (*N*-2-hydroxyethylpiperazine-*N*′-2-ethanesulfonic acid) was obtained from ICN (Madrid).

Physical Measurements. NMR spectra were recorded in DMSO-d_6 with either a 200 or 300 MHz spectrometer. ES^+ mass spectra were recorded on a Fisons VG Quatro spectrometer at the Servei d'Espectrometria de Masses (Universitat de Barcelona). Elemental analyses of C, H, N, and S were carried out at the Serveis Científico-Tècnics (Universitat de Barcelona). The atomic-force microscopy (AFM) images were obtained with a NanoScope III MultiMode AFM system from Digital Instruments, Inc. operating in tapping mode. Fluorescence microscopy was carried out with an Olympus E800 and a Nikon Eclipse E600 equipped with a UV2A filter. Electrochemical data were obtained by cyclic voltammetry under nitrogen at 25 °C using dry acetonitrile as the solvent and tetrabutylammonium hexafluorophosphate (0.1 M) as the supporting electrolyte. The redox half-wave potentials were referenced to an Ag/AgCl (in 3 M NaCl) electrode separated from the solution by a medium-porosity fritted disk. A platinum-wire auxiliary electrode was used in conjunction with a platinum-disk working electrode, Tacussel-EDI rotatory electrode (3.14 mm^2). Cyclic voltammograms of 5×10^{-4} M solutions of the samples in CH_2Cl_2 were recorded with a BioLogic Science Instruments SP-150 potentiostat.

Synthesis and Characterization. *N,N′-(o-Phenylene)bis(5-methoxysalicylideneimine),* ***1a.*** A solution of 2-hydroxy-5-methoxybenzaldehyde (0.6 g, 3.9 mmol) and 1,2-diaminobenzene (0.213 g, 2.0 mmol) in MeOH (8 mL) was stirred for 24 h. The mixture was then filtered, and the final product was obtained as orange solid in 72% yield. ^{1}H NMR (300 MHz, DMSO-d_6) δ: 12.26 (bs, 2H, OH), 8.87 (s, 2H, N=C−H), 7.86 (m, 2H, CH), 7.53−7.39 (m, 6H, CH), 6.91 (m, 2H, CH), 3.67 (s, 6H, CH_3). ^{13}C NMR (75 MHz, DMSO-d_6) δ: 163.27, 154.88, 152.26, 142.91, 128.19, 121.14, 119.96, 119.89, 118.00, 115.10, 55.97. HRMS-ESI-TOF: calcd, 376.15; found, [M + H^+] 377.15 . Anal. Calcd for $C_{22}H_{20}N_2O_4$: C, 70.20; H, 5.36; N, 7.44. Found: C, 70.22; H, 5.37; N, 7.46.

N,N′-(o-Phenylene)bis(5-bromosalicylideneimine), ***2a.*** A solution of 2-hydroxy-5-bromobenzaldehyde (0.487 g, 2.4 mmol) and 1,2-diaminobenzene (0.133 g, 1.2 mmol) in MeOH (10 mL) was stirred for 24 h. The mixture was then filtered, and the final product was obtained as an orange solid in 84% yield. ^{1}H NMR (300 MHz, DMSO-d_6) δ: 12.90 (bs, 2H, OH), 8.89 (s, 2H, N=C−H), 7.40−7.25 (m, 6H, CH), 7.02−6.84 (m, 4H, CH), 3.71 (s, 6H, CH_3). ^{13}C NMR (75 MHz, DMSO-d_6) δ: 162.66, 159.90, 142.46, 136.10, 134.20, 128.58, 121.88, 120.09, 119.60, 110.32. HRMS-ESI-TOF: calcd, 471.95; found, [M + H^+] 472.95. Anal. Calcd for $C_{20}H_{14}Br_2N_2O_4$: C, 50.66; H, 2.98; N, 5.91. Found: C, 50.68; H, 2.99; N, 5.93.

N,N′-(o-Phenylene)bis(5-nitrosalicylideneimine), ***3a.*** A solution of 2-hydroxy-5-nitrobenzaldehyde (0.403 g, 2.4 mmol) and 1,2-diaminobenzene (0.136 g, 1.2 mmol) in MeOH (25 mL) was stirred for 24 h. The mixture was then filtered, and the final product was obtained as an orange solid in 92% yield. ^{1}H NMR (300 MHz, DMSO-d_6) δ: 10.17 (bs, 2H, OH), 9.16 (s, 2H, N=C−H), 9.16 (s, 2H, CH), 8.73 (m, 2H, CH), 8.28−8.16 (m, 2H, CH), 7.71−7.47 (m, 4H, CH), 7.09−7.01 (m, 2H, CH). HRMS-ESI-TOF: calcd, 406.09; found, [M + H^+] 407.09. Anal. Calcd for $C_{20}H_{14}N_4O_6$: C, 59.12; H, 3.47; N, 13.79. Found: C, 59.18; H, 3.50; N, 13.81.

N,N′-(o-Phenylene)bis(5-methoxysalicylideneiminato)zinc(II), ***1b.*** A solution of 2-hydroxy-5-methoxybenzaldehyde (0.395 g, 2.6 mmol), 1,2-diaminobenzene (0.140 g, 1.3 mmol), and $Zn(OAc)_2{\cdot}2H_2O$ (0.307 g, 1.4 mmol) in MeOH (14 mL) was stirred for 24 h. The mixture was then filtered, and the final product was obtained as a yellow solid in 73% yield. ^{1}H NMR (300 MHz, DMSO-d_6) δ: 8.98 (s, 2H, N=C−H), 7.85 (m, 2H, CH), 7.33 (m, 2H, CH), 6.94−6.90 (m, 4H, CH), 6.64−6.61 (m, 2H, CH), 3.67 (s, 6H, CH_3). ^{13}C NMR (75 MHz, DMSO-d_6) δ: 168.12, 162.30, 147.56, 139.53, 127.25, 124.81, 124.20, 117.78, 116.52, 116.06, 55.67. HRMS-ESI-TOF: calcd, 438.06; found, [M + H^+] 439.06. Anal. Calcd for $C_{22}H_{18}N_2O_4Zn$: C, 60.08; H, 4.13; N, 6.37. Found: C, 60.12; H, 4.15; N, 6.38.

N,N′-(o-Phenylene)bis(5-bromosalicylideneiminato)zinc(II), ***2b.*** A solution of 2-hydroxy-5-bromobenzaldehyde (0.265 g, 1.3 mmol), 1,2-diaminobenzene (0.076 g, 0.7 mmol), and $Zn(OAc)_2{\cdot}2H_2O$ (0.344 g, 1.6 mmol) in MeOH (15 mL) was stirred for 24 h. The mixture was then filtered, and the final product was obtained as a yellow solid in 65% yield. ^{1}H NMR (300 MHz, DMSO-d_6) δ: 8.97 (s, 2H, N=C−H), 7.84 (m, 2H, CH), 7.58 (m, 2H, CH), 7.38 (m, 2H, CH), 7.27 (m, 2H, CH), 6.63 (m, 2H, CH). ^{13}C NMR (75 MHz, DMSO-d_6) δ: 171.11, 162.33, 139.36, 137.46, 136.62, 127.98, 125.66, 121.13, 116.92, 102.88. HRMS-ESI-TOF: calcd, 533.86; found, [M + H^+] 534.86. Anal. Calcd for $C_{20}H_{12}Br_2N_2O_2Zn$: C, 44.69; H, 2.25; N, 5.21. Found: C, 44.72; H, 2.26; N, 5.24.

N,N′-(o-Phenylene)bis(5-nitrosalicylideneiminato)zinc(II), ***3b.*** A solution of 2-hydroxy-5-nitrobenzaldehyde (0.372 g, 2.2 mmol), 1,2-diaminobenzene (0.119 g, 1.1 mmol), and $Zn(OAc)_2{\cdot}2H_2O$ (0.295 g, 1.2 mmol) in MeOH (10 mL) was stirred for 24 h. The mixture was then filtered, and the final product was obtained as a yellow solid in 70% yield. ^{1}H NMR (300 MHz, DMSO-d_6) δ: 8.39 (s, 2H, N=C−H), 7.79 (m, 2H, CH), 7.29−7.13 (m, 4H, CH), 6.67 (m, 2H, CH), 5.95 (m, 2H, CH). ^{13}C NMR (75 MHz, DMSO-d_6) δ: 177.15, 163.08, 156.97, 139.46, 134.82, 134.46, 128.89, 124.17, 119.00, 117.69. HRMS-ESI-TOF: calcd, 468.00; found, [M + H^+] 469.0. Anal. Calcd for $C_{20}H_{12}N_4O_6Zn$: C, 51.14; H, 2.57; N, 11.93. Found: C, 51.17; H, 2.59; N, 11.96.

Molecular Modeling and Semiempirical Calculations. The electronic structure and electronic transitions were calculated with the AM1 semiempirical method in structures previously optimized with the MM+ molecular mechanics method. Both of these methods were included in the software package HyperChem 7.0. (Hypercube, Inc.).[25]

dx.doi.org/10.1021/ic4004356 | *Inorg. Chem.* 2013, 52, 9245−9253

Atomic Force Microscopy Experiments. pBR322 DNA was heated before use at 60 °C for 10 min to obtain the open circular (OC) form. The stock solution is 1 mg/mL in a HEPES buffer solution. Each sample contains 1 μL of DNA pBR322 at a concentration of 0.25 μg/μL and a final volume of 50 μL. The amount of drug added was expressed as r_i (i.e., the ratio between the drug's molar concentration to the number of base pairs). All of the stock solutions were freshly prepared in milli-Q water with 2% DMSO.

UV–Vis Spectrophotometric Studies. The absorption titrations were performed by adding increasing amounts of ct-DNA (calf thymus DNA) to the complexes in Tris-HCl buffer (5 mM) and NaCl (50 mM) at pH 7.2. The concentration of ct-DNA was determined from the absorption intensity at 260 nm with a molar extinction coefficient of 6600 M^{-1} cm^{-1}. After the addition of DNA to the metal complex, the resulting solution was allowed to equilibrate at 25 °C for 2 min, after which time the absorption spectra were recorded.

Fluorescence Spectrophotometric Titrations. The relative binding affinities of the complexes to ct-DNA were studied with an ethidium bromine (EB)-bound ct-DNA solution in a 5 mM Tris-HCl and 50 mM NaCl buffer (pH 7.2). The fluorescence spectra were recorded at room temperature with excitation at 514 nm. The titration experiments were carried out with an EB–DNA solution containing 2.5×10^{-5} M EB, 1×10^{-5} M ct-DNA, and 75×10^{-3} μg μL^{-1} of the compounds.

Cytotoxicity Studies. For the cytotoxicity assays, 3T3 Balb/c cells were cultured in Dulbecco's modified Eagle's medium (DMEM, Sigma-Aldrich) containing 10% fetal calf serum (Hyclone), 2 mM glutamine (Sigma-Aldrich), and antibiotics (Sigma-Aldrich, 50 μg/mL of penicillin and 50 μg/mL of streptomycin). Thus, the cells were incubated for 24 h for correct adhesion. Afterward, solutions of the salophen were added to some wells, whereas a 0.2% solution of sodium dodecylsulfate (SDS) was added to the others for a positive control. The incubation was prolonged for a further 24 h. The cells were exposed to a range of concentrations from 2277 to 8.91 mM for **1b**, 1873 to 7.32 mM for **2b**, and 2132 to 8.34 mM for **3b** under 5% CO_2 at 37 °C. The viability was assessed by the MTT assay on the basis of the mitochondrial dehydrogenase enzyme's capability of hydrolyzing a bromide chromogen (3-(4,5-dimethylthiazol-2-yl)-2,5-diphenyltetrazolium bromide). The cells were washed with PBS (3×), and fresh medium was added together with a 5 mg/mL MTT solution and incubated for 2 h at 37 °C under a 5% CO_2 atmosphere. This compound shows a pale-yellow color in solution, and its conversion by the enzyme reduces the MTT to a formazan in the mitochondria of living cells, which is a crystallized, dark-blue compound that cannot cross the cell membrane.

Because of the low solubility of the compounds in water, a second cytotoxicity assay was carried out using DMSO (1%) as the solvent with the same concentrations of compounds that were previously assayed.

The data were statistically analyzed to calculate the 50% inhibition concentrations, IC_{50}, using the SPSS program (version 15 for Windows) and applying the Probit regression.

Genotoxicity Comet Assay. The genotoxicity study of the 3T3 Balb/c fibroblast cell line was performed via the comet assay according to the ASTM-E2186 guideline.[26]

Cells were cultured in 6-well flat-bottomed microtiter plates containing 2 mL of the cell suspension (~2×10^5 cells). After 24 h of incubation at 37 °C with 5% CO_2, the compound to be investigated was added. Only two doses were used for compound **1b**, 8.91 and 17.81 μM. For **2b**, 7.32, 14.65, 29.28, and 58.54 μM were used, and for **3b**, 16.67 and 33.33 μM were used. After 24 h of exposure, the 3T3 fibroblast cells were detached from the well with a 0.05% trypsin solution and collected by centrifugation. The cells were embedded in low-melting point 0.9% agarose (LMP-Gibco) prepared in Milli-Q water (18 MΩ) and layered on precoated slides. The slides were placed in lysing buffer (2.5 M NaCl, 100 mM Na_2EDTA, 10 mM Tris pH 10, and *N*-lauryl-sarcosine 1% (w/v) (Sigma) with 1% Triton X-100) for 1 h at 4 °C. The isolated DNA from the nuclei in the agarose gels was unwound for 40 min in electrophoresis buffer (1 mM Na_2EDTA and 300 mM NaOH, pH > 13). The SCGE slides were then electrophoresed for 30 min at 25 V and 300 mA at 4 °C. After neutralization with 400 mM Tris buffer (pH 7.5), the slides were dried at room temperature. For image analysis, the slides were hydrated and stained with 10 μL of DAPI at 14.28 μM. Nondamaged cells exhibit a spherical shape, whereas fragmented nucleoids migrate, forming a tail ("comet" shape). The nucleoid damage was quantified as the percentage of fluorescence in the tail. In the assay, the percentage of DNA in the tail was determined with respect to the intensity of the total DNA for 50 cells. The determination was obtained with the Comet Assay IV software, and the corresponding statistics were performed using the SPSS program (version 15 for Windows) by applying Mann–Whitney U statistics.

Preliminary Cellular-Uptake Studies. 3T3 Balb/c cells were exposed to a single concentration of compounds **1b–3b** of ca. 71.17, 58.54, and 66.63 μM, respectively, and they were observed on an inverted fluorescence microscope with two different filters (B2A and UV2A). The observations were carried out at different times: 15 and 30 min as well as 1, 1.5, 2, and 24 h after exposure.

DNA-Binding Studies in Cells. Preliminary experiments were carried out with free nucleoids in an agarose matrix. Fixed nucleotides were stained with concentrations of compounds **1b–3b** of ca. 113.88, 93.66, and 106.61 μM, respectively. Staining with DAPI (4′,6-diamidino-2-phenylindole, 14.28 μM), a well-known fluorescent stain that acts as a DNA minor-groove binder and DNA intercalator, at a concentration of 14.28 μM allowed us to obtain better microscopy images.

For the internalization of compounds, 3T3 cells were seeded onto a coverslip in a 24-well plate and grown overnight under normal growth conditions followed by incubation with **1b** at 30.29 μM, **2b** at 37.46 μM, and **3b** at 53.3 μM for an additional 3 h. Control cells were treated with an equivalent amount of DMSO. Cells were fixed with 4% formaldehyde in PBS for 30 min, washed (2×) with PBS, and permeabilized with 0.2% Triton X-100 in PBS for 5 min. The cells were washed 3× with cold PBS followed by incubation with Draq5 (10 μM) for 30 min at room temperature. Stained cells were washed 3× with cold PBS, mounted on a microscope slide with Mowiol mounting media, and visualized under a Leica TCS SP2 AOBS system (405 nm excitation laser diode for the complexes and 688 nm for Draq5). To detect molecules inside the cell, we performed a lambda scan with a wide range of wavelengths. With the *z* plain fixed inside the nucleus thanks to the Draq5 colocalization stain, pictures were taken at different wavelengths ranging from 405 to 600 nm. We selected different points within the cell and measured the intensity of the light emitted from each region.

RESULTS AND DISCUSSION

Synthesis and Characterization. Compounds **1a–3a** were prepared according to the standard procedure for salen and salophen ligands[27] using the appropriate substituted salicylaldehyde and 1,2-diaminobenzene as starting materials. The reactants were refluxed in methanol for 1 h, during which time the desired products precipitated as orange solids in pure form. A similar procedure was used for the synthesis of the corresponding Zn-salophen complexes **1b–3b** in the presence

Table 1. Absorption and Emission Data of Compounds 1a–3a and 1b–3b[a]

compound	absorption (nm) ($\varepsilon \times 10^{-3}$, M^{-1} cm^{-1})	emission (nm)[a]
1a (OMe)	274 (4.9), 354 (3.1)	
2a (Br)	268 (21.4), 341 (14.2)	
3a (NO_2)	279 (27.7), 404 (9.3)	
1b (OMe)	300 (10.4), 432 (7.2)	551
2b (Br)	290 (24.9), 400 (19.7)	507
3b (NO_2)	295 (37.1), 380 (39.6)	476

[a]Excitation at the lowest energy absorption band.

dx.doi.org/10.1021/ic4004356 | Inorg. Chem. 2013, 52, 9245–9253

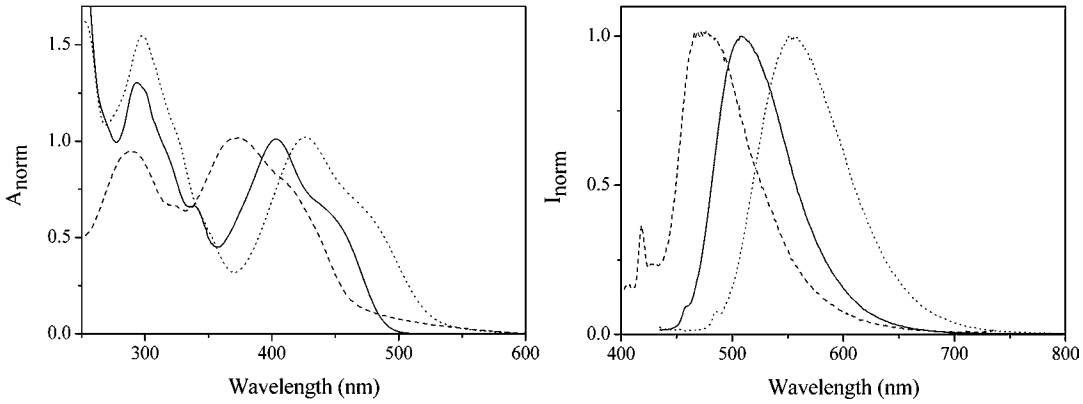

Figure 1. Normalized absorption (left) and emission spectra (right) of compounds **1b** (dotted line), **2b** (solid line), and **3b** (dashed line).

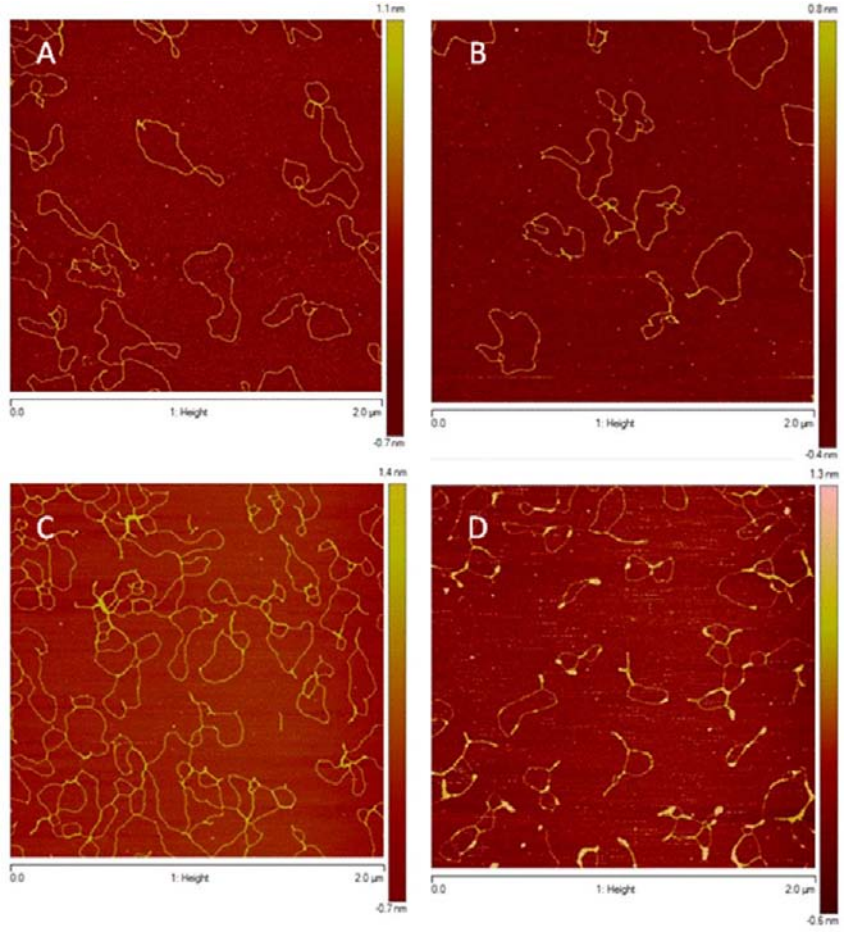

Figure 2. AFM image of pBR322 plasmid DNA (A) and pBR322 plasmid DNA incubated with **1b** (B), **2b** (C), and **3b** (D).

Table 2. Calculated Energy of the HOMO and LUMO Frontier Orbitals of Salophen Complexes 1b−3b and the DNA Nucleobases and HOMO−LUMO Energy Differences ($\Delta E = E_{LUMO}$(salophen) − E_{HOMO}(nucleobase))

compound	HOMO (eV)	LUMO (eV)	ΔE, G (eV)	ΔE, C (eV)	ΔE, A (eV)	ΔE, T (eV)
1b (OMe)	−7.95	−1.24	7.38	8.14	7.53	8.37
2b (Br)	−8.43	−1.47	7.15	7.91	7.3	8.14
3b (NO_2)	−9.20	−2.00	6.62	7.38	6.77	7.61
guanine	−8.62	−0.29				
cytosine	−9.38	−0.10				
adenine	−8.77	−0.11				
thymine	−9.61	−0.29				

dx.doi.org/10.1021/ic4004356 | *Inorg. Chem.* 2013, 52, 9245−9253

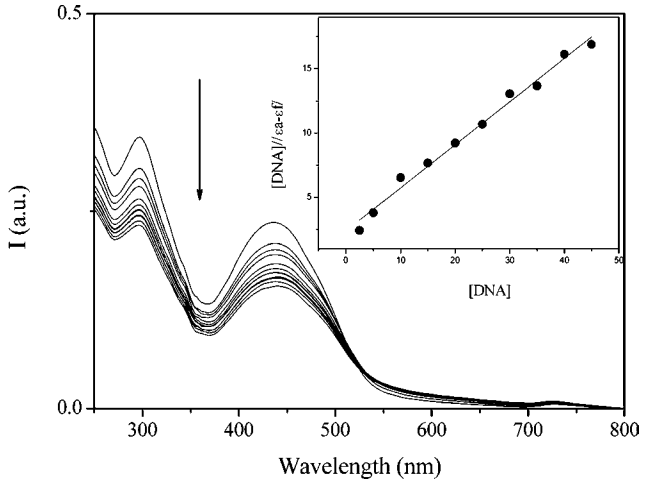

Figure 3. Electronic absorption spectra of complex **3b** in the absence and presence of increasing amounts of DNA. The inset shows a plot of $[DNA]/(\varepsilon_a - \varepsilon_f)$ vs [DNA].

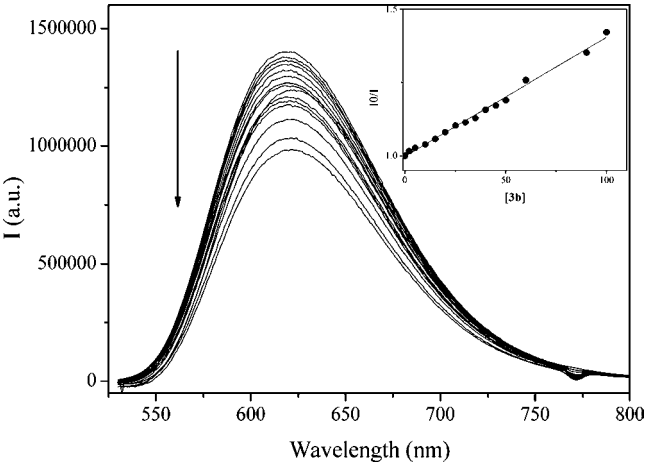

Figure 4. Emission spectra of ethidium bromide (EB) bound to DNA in the absence and presence of increasing amounts of **3b**. The inset shows the Stern–Volmer plot I_0/I vs [**3b**].

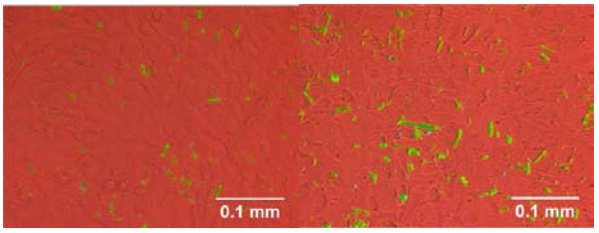

Figure 5. Fluorescence-microscopy images of 3T3 cells incubated for 24 h with 14.61 (left) and 29.28 μM (right) of compound **2b**. The pink tint represents the culture medium and green areas represent fluorescent compound **2b**.

Table 3. Estimated IC_{50} Values of 1b–3b in DMSO[a]

compound	IC_{50} (μM, DMSO)	(LCI, UCI)
1b	71	NP
2b	89	(76, 102)
3b	1073	(943, 1236)

[a]LCI: lower confidence interval. UCI: upper confidence interval (95% confidence). NP: not possible to calculate.

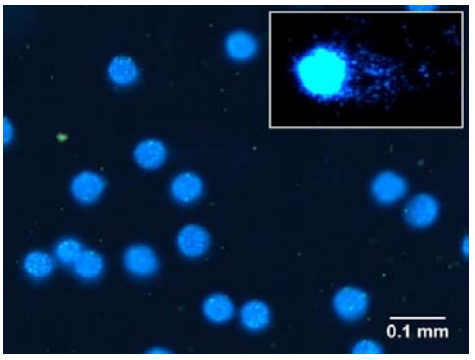

Figure 6. Microscopy image (20×) of cells in a DAPI-staining solution in the presence of compound **1b** at 17.81 μM using a UV2A fluorescence filter. The comet shape is not observed. The inset shows the comet shape observed for the MMS positive control as a reference.

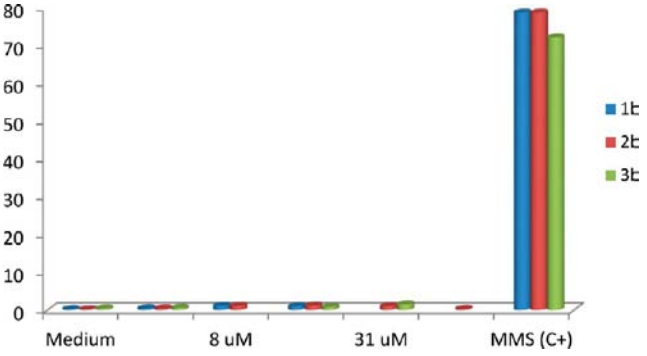

Figure 7. Histogram of the genotoxicity assay results for compounds **1b–3b** with 3T3 cells. Medium = vehicle control (1% DMSO) and C+ = positive control (MMS).

of a stoichiometric quantity of zinc acetate dihydrate. All of the compounds were obtained in moderate–good yields (ca. 70–90%).

Characterization by different spectroscopic techniques and spectrometry verified the formation of the ligands and complexes. ^{1}H NMR shows the expected signals for the salophen derivatives. The protons are clearly affected by metal coordination (e.g., whereas the signal of phenolic protons obviously disappears, imine and aromatic protons are ca. 0.5–1 ppm upfield shifted, respectively). HRMS-ESI-TOF led us to identify unequivocally the products because they display the corresponding protonated molecular peak in all cases.

Optical Properties. Absorption and emission spectra of the **1a–3a** ligands and respective Zn(II) complexes **1b–3b** were studied, and the relevant photophysical data are summarized in Table 1 and Figures 1 and S1.

Uncomplexed salophen compounds **1a–3a** show broad, unstructured absorption bands in the 270–400 nm region with a similar pattern for the reported salophen derivatives (Figure S1). We have performed theoretical semiempirical calculations, and as already observed for similar derivatives[28] the observed transitions are predominantly π–π^* (Figures S2–S4). No significant luminescence was observed for any of them.

Coordination to Zn(II) metal (complexes **1b–3b**) gives absorption patterns similar to those observed for the corresponding free ligands but generally shifted to lower energies. Excitation at the lower-energy band gives rise to fluorescence broad bands centered in the 475–550 nm region. The donor/acceptor electronic character of the substituents on

dx.doi.org/10.1021/ic4004356 | Inorg. Chem. 2013, 52, 9245–9253

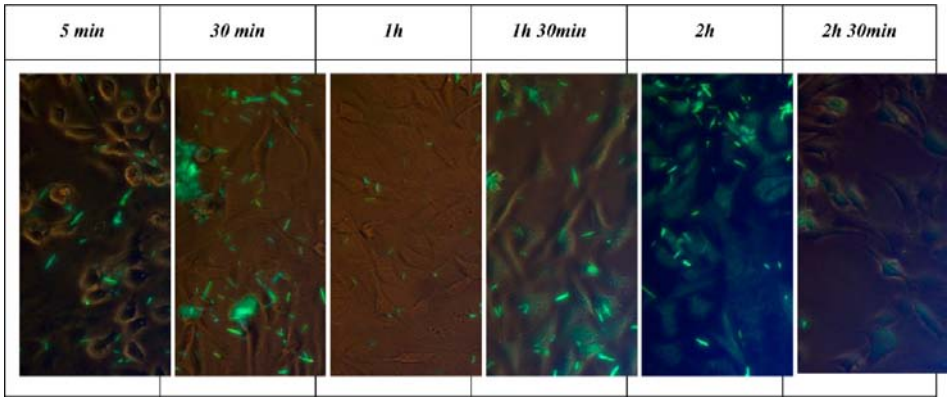

Figure 8. Fluorescence microscopy image of 3T3 fibroblast cells incubated with **3b** at 66.63 μM for different amounts of time (20× and UV2A filter).

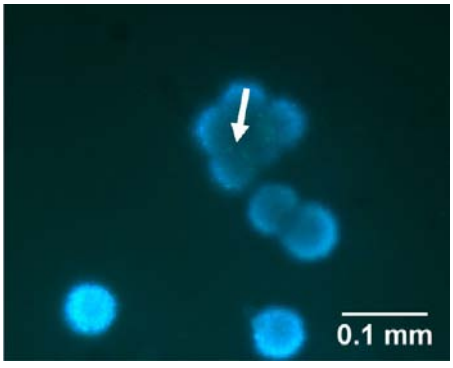

Figure 9. Fluorescence microscopy image (20×) of nucleoids incubated with compound **1b** (green dots, 113.88 μM) in the presence of DAPI with the UV2A filter.

the salophen ligands is reflected in the energy of both the absorption and emission bands, showing the energy trend OMe < Br < NO_2 (i.e., the higher the electron-donating character, the lower the energy of the observed transition).

AFM Studies. Recently, the AFM technique has been shown to be a very useful tool to explore the interactions of similar Zn(II)-salophen complexes with DNA.[19] In the present work, we used this technique to investigate the effect of substituents with different electronic characteristics on the interaction with DNA.

Free pBR322 plasmid DNA was incubated for 24 h with aqueous solutions (2% DMSO) of **1a**−**3a** and **1b**−**3b**. At the end, no significant interactions were observed between the DNA and all the three salophen ligands (Figure S5). The open circle (OC) form of DNA is just slightly perturbed upon incubation with nitro-salophen ligand **3a**, and no effect is observed with **1a** and **2a**. Instead, incubation with zinc complexes induces much more significant effects in the DNA structure, in particular in the presence of **3b** (Figure 2). The initial OC form of the DNA disappears almost completely in the presence of this complex, giving rise to the formation of mixed toroidal and plectonemic supercoils as well as to complete plectonemic supercoiling. It is likely that such behavior is due to the intercalation of the molecules into the DNA, a phenomenon already observed by us with similar zinc-salophen complexes.[19] However, the OC form of the DNA is almost unaffected by the presence of **1b** and **2b** (Figure 2).

Because the only difference in the three complexes is the nature of the substituents, the degree of the interaction with DNA might be related to their electron-withdrawing/electron-donating character. The complex that visibly interacts with DNA is the one containing the strongest electron-withdrawing substituent, **3b**. Consequently, the observed effect can be ascribed to the Lewis acid−base interaction that occurs between the electron-poor salophen (electronic density is withdrawn by the presence of the nitro substituent) and the DNA nucleobases (most likely guanine and adenine).

To support such a hypothesis, the compounds have been modeled using the AM1 method in structures previously optimized with MM+ molecular mechanics (both are included in the software package HyperChem 7.0).[25] The energies of the HOMO and LUMO orbitals of **1b**−**3b** were analyzed with respect to those of the frontier orbitals of the DNA nucleobases

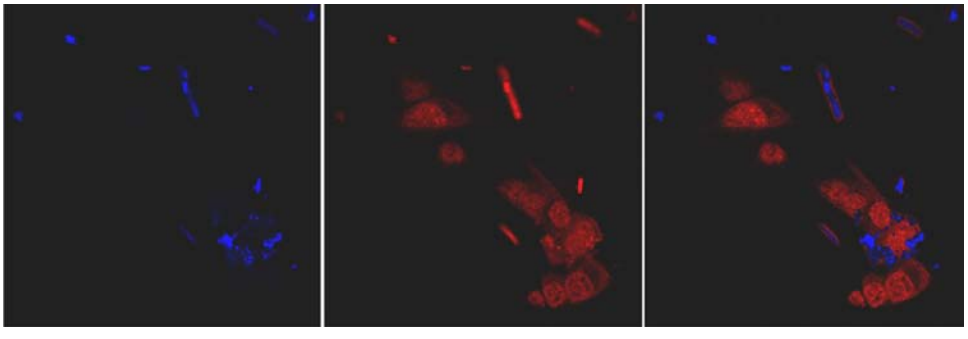

Figure 10. Fluorescence confocal microscopy image of 3T3 cells incubated with compound **3b** (106.61 μM, blue color, left), Draq5 (red-color stained nuclear DNA, middle), and the superimposed images (right). The incubation time was 3 h.

dx.doi.org/10.1021/ic4004356 | *Inorg. Chem.* 2013, 52, 9245−9253

and reported in Table 2. The energy differences between the HOMO of the different nucleobases and the LUMO of the different salophen complexes, ΔE, are also included for clarity. We should point out that this is an approximation because DNA contains stacks of nucleobases rather than individual nucleobases, and the HOMO and LUMO energies could be modified accordingly. In fact, stacks of guanine bases have been found to have an even lower ionization potential than individual guanine bases, and the presence of metal complexes could have an important electronic role of pulling electrons from the coordinated aromatic ligands, making them increasingly electron-deficient and therefore much more likely to be involved in substantial $\pi-\pi$ interactions with G-quartets and nucleobases.[11]

As shown in Table 2, the lowest energy HOMO and LUMO orbitals of the salophen complexes are those of nitro derivative **3b**. The complex acts as a Lewis acid; therefore, the suggested interaction with DNA can be associated to a charge-transfer process from the DNA bases to the salophen complex. From the data in Table 2, it appears that purine nucleobases favor this process because the ΔE (HOMO (nucleobase) → LUMO (**3b**)) are the lowest (ΔE values G and A for **3b** in Table 2). In particular, guanine should provide the lowest transition barrier, which is in agreement with the fact that its ionization potential is the lowest among the four nucleobases.[29] Therefore, it is the complex that is more susceptible to involvement in the charge-transfer interaction that contributes to the stabilization of the **3b**−nucleobase adduct. Consequently, the calculations are in agreement with the AFM data that indicate that **3b** was the only complex that strongly interacts with DNA.

We also measured the redox potentials of complexes **1b**−**3b**. The values are $E^0 = -0.71$, -0.59, and -0.35 V, respectively. From these data, it suggests that the strongest oxidant is nitro-derivative **3b**, which should be involved in the highest net redox potential value of these electronic processes, E^0 ($E^0 = E^0_{ox}$(nucleobase) + E^0_{red}(complex)).

DNA-Binding Studies by Absorption and Emission Titrations. Absorption spectra of the complexes were recorded after the addition of increasing amounts of DNA (Figures 3, S6, and S7). A decrease in molar absorptivity (hypochromism) was observed for the three complexes, and a slight bathochromism (ca. 4 nm) was observed for **3b**.

The binding affinity constants, K_b, of the complexes with DNA could be determined quantitatively using the following equation[30]

$$[\mathrm{DNA}]/(\varepsilon_a - \varepsilon_f) = [\mathrm{DNA}]/(\varepsilon_b - \varepsilon_f) + 1/K_b(\varepsilon_b - \varepsilon_f)$$

where [DNA] is the concentration of ct-DNA in base pairs, and ε_a, ε_f, and ε_b are the apparent extinction coefficients corresponding to A_{obs}/[complex], which is the extinction coefficient for the unbound compound and the extinction coefficient for the compound in the fully bound form, respectively.

The binding constants for **1b**−**3b** were calculated to be 8.8×10^4, 1.3×10^5, and 1.5×10^5 M^{-1}, respectively. The values are comparable with those reported recently by us for similar Zn-salophen complexes (1.7×10^5 and 1.6×10^5 M^{-1}).[19]

Further experiments were carried out using EB, a known intercalating agent, to establish if the interactions with DNA (especially in the case of **3b**) can be due to an intercalation mode. EB is nonemissive in phosphate buffer (pH 7.2) because of fluorescence quenching of free EB by solvent molecules, but it emits intensely in the presence of DNA as the result of its intercalation between adjacent DNA base pairs. When a second species is added, it can compete with EB for DNA binding sites, causing a decrease in the fluorescence intensity. The quenching is due to the decrease of the number of available DNA binding sites. Therefore, EB is used as a common fluorescent probe for DNA structure that is able to provide information about the mode and process of single species binding to DNA.[31]

Fluorescence titrations showed that only **3b** can replace some of the EB binding sites, inducing a quenching effect (Figures 4, S8, and S9). The observed quenching of DNA−EB in the presence of **3b** follows the Stern−Volmer equation

$$\frac{I_0}{I} = 1 + K_q[\mathrm{Q}]$$

where I_0 and I represent the emission intensity in the absence and presence of quencher, respectively, K_q is a linear Stern−Volmer quenching constant, and [Q] is the quencher concentration (i.e., the concentration of the zinc-salophen derivatives in our study). This equation is considered for static quenching because this is the expected process for the displacement of EB by the salophen complexes. Hence, the obtained I_0/I versus [Q] plot follows a linear pattern that allowed us to calculate a K_q value of 9.4×10^3 M^{-1}, which is the same value previously reported for similar Zn-salophen complexes.[19]

Absorption and emission experiments are indicative of a likely intercalation mode of the complex into double helix ct-DNA. Nevertheless, the association constant between DNA and EB is two orders of magnitude higher than the one calculated for our complex, showing that EB is a stronger intercalating agent.

The different values obtained for K_b and K_q are due to the different chemical processes under study. From UV−vis spectroscopic titrations we can calculate the association constants between the compounds and DNA, whereas spectrofluorimetric titrations let us to obtain the quenching constant for the EB-displacement process. Thus, the process under study is characterized by an apparent constant defined by the equation $K_{app} = K_{ass}/K_{EB}[\mathrm{EB}]$. By taking into consideration that K_{EB} is 1×10^7 M^{-1}, the corresponding K_b values obtained from the luminescence experiments are ca. 1.5×10^5 M^{-1}, which is exactly the same value calculated by the absorption experiment.

The experiments were not carried out with the ligands because no significant interactions were observed with any of them in the AFM studies.

Cytotoxicity Studies. Before studying the in vitro internalization of the compounds using 3T3 cells and the interactions of the complexes with DNA in these assays, it was necessary to assess the toxicity of the compounds. Cytotoxicity was evaluated by MTT experiments following a protocol detailed in the Experimental Section. Incubated cells were seeded in 96-well plates at a 10^5 cell/mL density for 24 h. Seeded cell wells without MTT were used as blank experiments to evaluate the effect (cell binding) of the complexes on the 3T3 cells. After 24 h of incubation, the cells were analyzed by fluorescence microscopy using a UV2A filter.

Fluorescence-microscopy images of the cells incubated with two different concentrations of the complexes show that an increase in the concentration of the salophen compound does not seem to reduce the number of incubated cells; therefore, no significant cytotoxicity was expected for any of them (Figure 5).

dx.doi.org/10.1021/ic4004356 | Inorg. Chem. 2013, 52, 9245−9253

The cytotoxicity has been evaluated with respect to negative control DMSO (1%) using SDS as a positive control (with a growth-inhibition value above 90%). It is most likely that above a 70 μM concentration the cytotoxicity does not originate exclusively from the interaction between the metal-containing compounds and the DNA but also from the excess of **1b** and **2b** that covers the cells (outside the cell membrane, Figure S10), which does not allow for proper growth. A very large amount (>500 μM) of **3b** is required to induce cell death. By considering that for concentrations higher than ca. 60 μM the compounds do not seem to induce cells death, the growth-inhibition effects observed may be directly due to a cell-recovery effect by the compounds (outside the cell membrane) and not to interactions between the complexes and organelles or DNA. The growth-inhibition percentages obtained at different concentrations allowed the calculation of the 24 h IC_{50} values using a Probit regression method included in the SPSS (Statistical Package for the Social Sciences) program, version 15 for Windows (Table 3 and Figure S11). These values are calculated from 19 independent repetitions.

The estimated IC_{50} values are lower (mainly for **1b** and **2b**) than those previously obtained for similar Zn-salophen derivatives containing two isopropyl groups in the 3,3′ positions (1.29 and 1.85 mM in water).[19] An increase in the electron-withdrawing effect (poorer electronic character of the salophen complex ligand) leads to an increase of the calculated IC_{50} (less cytotoxicity).

However, the IC_{50} values of the parent ligands (**1a**−**3a**) have been also calculated for comparison purposes, and the corresponding values are 158.71, 160.99, and 595.96 μM, respectively. All of these values are clearly different from those of the corresponding complexes, indicating the relevant role of the metal on the cytotoxic activity and the different effect of the nitro substituent with respect to that of the methoxy and bromide substituents.

Genotoxicity: Comet Assays. Comet assays were carried out with 3T3 fibroblast cells to detect the interaction of the complexes with DNA in the cells (experiments have been undertaken at different concentrations that are always below the calculated IC_{50}).

This experiment is commonly applied to detect DNA fragmentation in individual cells, which allows the assessment of genotoxic effects or antigenotoxic (protective) activity against a clastogenic challenge (i.e., chromosome breakage).[32] Nondamaged cells will exhibit a spherical shape, whereas fragmented nucleoids will migrate, forming a tail with a comet shape. The nucleoid damage was quantified as the percentage of a cells fluorescence observed in the tail. A comparison of the results with a genotoxic positive control (400 μM solution of methyl methanesulfonate, MMS) and with DMSO (1%) as a vehicle control revealed that the nucleoid is clearly not damaged because the spherical shape of the nucleoid is not modified (Figures 6 and 7).

The corresponding images displayed in Figures 6 and 7 clearly show that the nucleus is stained by DAPI and that the zinc complexes seem to enter the cells but without binding specifically to the nucleus. The observed effect is slightly inferior to that previously obtained for similar Zn-salophen complexes.[19]

All of these results demonstrate a clear effect of the electronic character of the substituent in in vitro studies, but according to the first studies carried out in cells, this effect does not seem to be observed in this biological medium. Nevertheless, the effect of the substituents can be used to modulate molecular recognition processes. Work along this line is in progress.

Preliminary Cellular-Uptake Studies. Cellular uptake studies were therefore carried out using 3T3 fibroblasts (connective tissue cells). After cells were incubated with **1b**−**3b** (71.17, 58.54, and 66.63 μM, respectively), the cultures were washed, and the cells were observed under an inverted fluorescence microscopy. Internalization seems to become evident at 1.5 h (Figure 8), but this observation is not homogenously extended to all of the cells.

DNA Binding. Compounds **1b**−**3b** were incubated with fixed nucleoids in an agarose matrix in at concentrations of 113.88, 93.66, 106.61 μM, respectively. The use of lower-concentration solutions seems to indicate nucleoid−compounds interaction, although it was difficult to localize them within the cells. DAPI (4′,6-diamidino-2-phenylindole) was also included in each sample in a clearly lower concentration (5 μg/mL) because it is a well-known fluorescent stain that acts as a DNA minor-groove binder and DNA intercalator (exhibiting an emission at 461 nm when it is excited at 358 nm), and its presence allowed us to identify the presence of the complexes in the cells and to obtain better microscopy images because more intensely DAPI-stained regions indicate more condensed DNA and vice versa.[33] Although these experiments let us to detect the presence of all three salophen complexes, they do not interact with the nucleus in the same way. Fluorescence microscopy images allowed us to identify the presence of **1b** and **3b** in the nucleus as small green dots (Figures 9 and S11), but the localization of **2b** is not so clear (Figure S12).

To analyze further these data, colocalization living-cell internalization was investigated using Draq5 as the fluorochrome. This is a far-red emitting fluorescent DNA dye is used for permeabilized and fixed live-cell analysis that can be used in combination with other common fluorophores. In the present case, the Draq5 staining proved to be appropriate because its red emission could be clearly separated from that of the zinc-salophen derivatives (observed at higher energies). Thus, 3T3 cells were stained with Draq5, and the emissions were observed by fluorescence confocal microscopy at 688 nm for Draq5 and at 500 nm for the complexes. Interestingly and in agreement with previous data (e.g., AFM, luminescence, redox potentials, etc.), we observed the presence of complex **3b** in the nucleus (Figures 10 and S13). In contrast, no traces of compounds **1b** and **2b** were detected. Images of cells stained by zinc complex **3b** (Figure 10, left) and with Draq5 (Figure 10, middle) are superimposed in Figure 10, right and indicate that the red staining resulting from Draq5 is colocalized with that corresponding to salophen complex **3b**, which is a definitive proof that this is the only complex of this series that interacts with DNA.

■ CONCLUSIONS

The present study of the biological properties of a series of salophen Zn(II) complexes clearly shows that the Lewis acid character of the complexes strongly affects the interaction with DNA in in vitro studies. Variation in the electronic properties of the substituents at the 5,5′ positions seems to modulate the strength of such interactions. In particular, the presence of the electron-withdrawing nitro substituents, increasing the electrophilic character of the metal center, generates the strongest interaction with plasmid DNA. Similar studies performed on the uncomplexed salophen ligands do not evidence any

dx.doi.org/10.1021/ic4004356 | Inorg. Chem. 2013, 52, 9245−9253

significant interaction even in the case of the nitro derivative, further highlighting the role played by zinc.

Semiempirical calculations together with cyclic voltammetry measurements suggest that this interaction can be also related to the lowest ΔE (HOMO (nucleobase) → LUMO (**3b**)) and thus a more favored charge-transfer process. Hence, our studies indicated that interaction with DNA can be modulated by changing the substituents of the salophen skeleton.

However, it has been observed that none of the complexes present significant cytotoxicity in cells. They are able to enter the cells, and **3b** in particular goes into the nucleus. Thus, they can be regarded as potential candidates for use as fluorescence markers.

■ ASSOCIATED CONTENT

Ⓢ Supporting Information

Absorption spectra of compounds **1a**−**3a** in ethanol; calculated orbitals involved in the lowest energy absorption transitions of compounds **1a**−**3a**; AFM image of pBR322 plasmid DNA alone and incubated with **1a**−**3a**; electronic absorption spectra of complexes **1b** and **2b** in the absence and presence of increasing amounts of DNA; emission spectra of ethidium bromide (EB) bound to DNA in the absence and presence of increasing amounts of **1b** and **2b**; fluorescence-microscopy images of 3T3 cells incubated with compound **2b**; cytotoxicity dose responses of metal complexes in 3T3 cells for compounds **1b**−**3b**; fluorescence microscopy image of nucleoids incubated with compound **2b** and **3b**; fluorescence confocal microscopy image of 3T3 incubated cells with Draq5 and compounds **1b** and **2b**. This material is available free of charge via the Internet at http://pubs.acs.org.

■ AUTHOR INFORMATION

Corresponding Author

*E-mail: antonella.dallacort@uniroma1.it (A.D.C.); E-mail: laura.rodriguez@qi.ub.es, Tel: +34 934039130, Fax: +34 934907725 (L.R.).

Notes

The authors declare no competing financial interest.

■ ACKNOWLEDGMENTS

The support and sponsorship provided by COST Action CM1005 is acknowledged. We are also grateful to the Ministerio de Ciencia e Innovación of Spain (project CTQ2012-31335) and Fundação para a Ciência e Tecnologia of Portugal (PTDC/QUI-QUI/112597/2009). We thank Drs. Lidia Bardia and Julien Collombelli from IRB-Barcelona for fruitful discussions.

■ REFERENCES

(1) Jacobsen, E. N.; Zhang, W.; Guler, M. L. *J. Am. Chem. Soc.* **1991**, *113*, 6703.
(2) Haak, R. M. S.; Wezenberg, J.; Kleij, A. W. *Chem. Commun.* **2010**, *46*, 2713.
(3) Venkataramanan, N. S.; Kuppuraj, G.; Rajagopal, S. *Coord. Chem. Rev.* **2005**, *249*, 1249.
(4) (a) Dalla Cort, A.; Mandolini, L.; Schiaffino, L. *Chem. Commun.* **2005**, 3867. (b) Dalla Cort, A.; Pasquini, C.; Schiaffino, L. *Supramol. Chem.* **2007**, *19*, 79. (c) Dalla Cort, A.; Mandolini, L.; Schiaffino, L. *J. Org. Chem.* **2008**, *73*, 9439.
(5) Bhattacharya, S.; Mandal, S. S. *Chem. Commun.* **1996**, 1515.
(6) Czlapinski, J. L.; Sheppard, T. L. *J. Am. Chem. Soc.* **2001**, *123*, 8618.
(7) Muller, J. G.; Paikoff, S. J.; Rokita, S. E.; Burrows, C. J. *J. Inorg. Biochem.* **1994**, *54*, 199.
(8) Routier, S.; Vezin, H.; Lamour, E.; Bernier, J. L.; Catteau, J. P.; Bailly, C. *Nucleic Acids Res.* **1999**, *27*, 4160.
(9) Gust, R.; Ott, I.; Posselt, D.; Sommer, K. *J. Med. Chem.* **2004**, *47*, 5837.
(10) Reed, J. E.; Arola Arnal, A.; Neidle, S.; Vilar, R. *J. Am. Chem. Soc.* **2006**, *128*, 5992.
(11) Campbell, N. H.; Abd Karim, N. H.; Parkinson, G. N.; Gunaratnam, M.; Petrucci, V.; Todd, A. K.; Vilar, R.; Neidle, S. *J. Med. Chem.* **2012**, *55*, 209.
(12) Ansari, K. I.; Grant, J. D.; Woldemaram, G. A.; Kasiri, S.; Mandal, S. S. *Org. Biomol. Chem.* **2009**, *7*, 926.
(13) Woldemaram, G. A.; Mandal, S. S. *J. Inorg. Biochem.* **2008**, *102*, 740.
(14) Ansari, K. I.; Grant, J. D.; Kasiri, S.; Woldemaram, G. A.; Shrestha, B.; Mandal, S. S. *J. Inorg. Biochem.* **2009**, *103*, 818.
(15) Dalla Cort, A.; De Bernadin, P.; Forte, G.; Yafteh Mihan, F. *Chem. Soc. Rev.* **2010**, *39*, 3863.
(16) Hille, A.; Ott, I.; Kitanovic, A.; Kitanovic, I.; Alborzinia, H.; Lederer, E.; Wölfl, S.; Metzler-Nolte, N.; Schäfer, S.; Sheldrick, W. S.; Bischof, C.; Schatzschneider, U.; Gust, R. *J. Biol. Inorg. Chem.* **2009**, *14*, 711.
(17) Ansari, K. I.; Kasiri, S.; Grant, J. D.; Mandal, S. S. *Dalton Trans.* **2009**, 8525.
(18) Alptürk, O.; Rusin, O.; Fakayode, S. O.; Wang, W.; Escobedo, J. O.; Warner, I. M.; Crowe, W. E.; Král, V.; Pruet, J. M.; Strongin, R. M. *Proc. Natl. Acad. Sci. U.S.A.* **2006**, *103*, 9756.
(19) Brissos, R.; Ramos, D.; Lima, J. C.; Yafteh Mihan, F.; Borràs, M.; de Lapuente, J.; Dalla Cort, A.; Rodríguez, L. *New J. Chem.* **2013**, *37*, 1046.
(20) Arola-Arnal, A.; Benet-Buchholz, J.; Neidle, S.; Vilar, R. *Inorg. Chem.* **2008**, *47*, 11910.
(21) Hai, Y.; Chen, J.-J.; Zhao, P.; Lv, H.; Yu, Y.; Xu, P.; Zhang, J.-L. *Chem. Commun.* **2011**, *47*, 2435.
(22) Pascu, S. I.; Waghorn, P. A.; Conry, T. D.; Lin, B.; Betts, H. M.; Dilworth, J. R.; Sim, R. B.; Churchill, G. C.; Aigbirhio, F. I.; Warren, J. E. *Dalton Trans.* **2008**, 2107.
(23) Gao, Y.; Wu, J.; Li, Y.; Sun, P.; Zhou, H.; Yang, J.; Zhang, S.; Jin, B.; Tian, Y. *J. Am. Chem. Soc.* **2009**, *131*, 5208.
(24) Ansari, K. I.; Kasiri, S.; Grant, J. D.; Mandal, S. S. *J. Biomol. Screening* **2011**, *16*, 26.
(25) *HyperChem*, version 7.5; Hypercube, Inc.: Gainsville, FL.
(26) *Standard Guide for Determining DNA Single-Strand Damage in Eukaryotic Cells using the Comet Assay*; ASTM Technical Bulletin E2186; ASTM International: West Conshohocken, PA, 2003.
(27) Singer, A. L.; Atwood, D. A. *Inorg. Chim. Acta* **1998**, *277*, 157.
(28) Cano, M.; Rodríguez, L.; Lima, J. C.; Pina, F.; Dalla Cort, A.; Pasquini, C.; Schiaffino, L. *Inorg. Chem.* **2009**, *48*, 6229.
(29) Mc Govern, D. A.; Doorley, G. W.; Whelan, A. M.; Parker, A. W.; Towrie, M.; Kelly, J. M.; Quinn, S. J. *Photochem. Photobiol. Sci.* **2009**, *8*, 542.
(30) Wolfe, A.; Shimer, G. H., Jr; Meehan, T. *Biochemistry* **1987**, *26*, 6392.
(31) Lippard, S. J. *Acc. Chem. Res.* **1978**, *11*, 211.
(32) Barenys, M.; Macia, N.; Camps, L.; de Lapuente, J.; Gómez-Catalan, J.; González-Linares, J.; Borràs, M.; Rodamilans, M.; Llobet, J. M. *Toxicol. Lett.* **2009**, *191*, 40.
(33) Ansari, K. I.; Mishra, B. P.; Mandal, S. S. *Biochim. Biophys. Acta* **2008**, *1779*, 66.